

Rochester Institute of Technology

RIT Scholar Works

Theses

5-2020

Radar-Aware Transmission and Scheduling for Cognitive Radio Dynamic Spectrum Access in the CBRS Radio Band

Dennis P. Bleier
dpb7341@rit.edu

Follow this and additional works at: <https://scholarworks.rit.edu/theses>

Recommended Citation

Bleier, Dennis P., "Radar-Aware Transmission and Scheduling for Cognitive Radio Dynamic Spectrum Access in the CBRS Radio Band" (2020). Thesis. Rochester Institute of Technology. Accessed from

This Thesis is brought to you for free and open access by RIT Scholar Works. It has been accepted for inclusion in Theses by an authorized administrator of RIT Scholar Works. For more information, please contact ritscholarworks@rit.edu.

**Radar-Aware Transmission and Scheduling for
Cognitive Radio Dynamic Spectrum Access in the
CBRS Radio Band**

DENNIS P. BLEIER

Radar-Aware Transmission and Scheduling for Cognitive Radio Dynamic Spectrum Access in the CBRS Radio Band

DENNIS P. BLEIER

May 2020

A Thesis Submitted
in Partial Fulfillment
of the Requirements for the Degree of
Master of Science
in
Computer Engineering

RIT | Kate Gleason College of
Engineering

Department of Computer Engineering

Radar-Aware Transmission and Scheduling for Cognitive Radio Dynamic Spectrum Access in the CBRS Radio Band

DENNIS P. BLEIER

Committee Approval:

Dr. Andres Kwasinski *Advisor* Date
Department of Computer Engineering

Dr. Andreas Savakis Date
Department of Computer Engineering

Dr. Alexander Loui Date
Department of Computer Engineering

Acknowledgments

I would like to thank my advisor, Dr. Andres Kwasinski, for his support and guidance throughout the project; Dr. Alexander Loui and Dr. Andreas Savakis for being members of the committee; and the Department of Computer Engineering for letting me take part in this research.

I would like to dedicate this work to my family and friends. Without your support I would not have been able to complete this work.

Abstract

Use of the wireless spectrum is increasing. In order to meet the throughput requirements, Dynamic Spectrum Access is a popular technique to maximize spectrum usage. This can be applied to the Citizen Broadband Radio Service (3550-3700MHz), a band recently opened by the Federal Communications Commission for opportunistic access. This radio band can be accessed as long as no higher priority users are interfered with. The top priority users are called incumbents, which are commonly naval radar. Naval radars transmit a focused beam that can be modelled as a periodic function. Lower tier users are prohibited from transmitting when their transmissions coincide and interfere with the radar beam. The second and third tier users are called Priority Access Licensees and General Authorized Access, respectively. Lower tier users must account for the transmission outage due to the presence of the radar in their scheduling algorithms. In addition, the scheduling algorithms should take Quality of Service constraints, more specifically delay constraints into account. The contribution of this thesis is the design of a scheduling algorithm for CBRS opportunistic access in the presence of radar that provides Quality of Service for users, consider different traffic needs.

This was implemented using the ns-3 discrete-event network simulator to simulate an environment with a radar and randomly placed radios using LTE-U to opportunistically transmit data. The proposed algorithm was compared against the Proportional Fair algorithm and a Proportional Fair algorithm with delay awareness. Performance was measured with and without fading models present. The proposed algorithm better balanced Quality of Service requirements and minimized the effect of transmission outage due to presence of the radar.

Contents

Signature Sheet	i
Acknowledgments	ii
Dedication	iii
Abstract	iv
Table of Contents	v
List of Figures	vii
List of Tables	viii
Acronyms	ix
1 Introduction	1
1.1 Introduction	1
1.2 Background	2
1.3 Previous Work	7
1.4 Motivation	10
1.5 Novel Contribution	10
2 System Setup	11
2.1 Physical Layout	11
2.2 Channel Characteristics	12
2.3 LTE and Internet Protocol	13
2.4 Radar Modelling	14
3 Radar-Aware Transmission and Scheduling	16
3.1 Radar-Aware Transmission and Scheduling	16
4 Results	19
4.1 Experimental Setup	19
4.1.1 NS-3 Setup	19
4.1.2 Design of Experiments	20

CONTENTS

4.2	No Fading Results	21
4.2.1	The Process to Final Values	27
4.3	Fading Results	29
4.4	Overall Result	32
4.5	Assumptions	33
5	Conclusions and Future Work	34
5.1	Conclusion	34
5.2	Future Work	34
	Bibliography	36

List of Figures

1.1	NS-3 LTE Radio Protocol Stack for eNodeB	4
1.2	Reprinted from 3GPP TS 36.213 [1]	5
1.3	Radar Beam Pattern at 60 RPM	8
2.1	User Equipment and EnodeB Layout	12
2.2	Network Topology of Simulated Network	13
2.3	Radar Beam Observed at Different Locations	15
4.1	LTE-EPC Stack in NS-3 [2]	20
4.2	Histograms of Proportional Fair No Fading	24
4.3	Histograms of Proportional Fair Delay Aware No Fading	25
4.4	Histograms of Proposed Algorithm No Fading Traffic	26
4.5	Histogram of Proportional Fair Fading	31

List of Tables

2.1	QCI Information Used in Simulation	14
4.1	No Fading System Parameters	22
4.2	NGBR_VID_VOICE_GAME Performance Without Fading	22
4.3	GBR_CONV_VOICE Performance Without Fading	23
4.4	GBR_GAMING Performance Without Fading	23
4.5	GBR_NON_CONV_VID Performance Without Fading	23
4.6	NGBR_VID_TCP Performance Without Fading	23
4.7	NGBR_VID_VOICE_GAME Performance	27
4.8	GBR_CONV_VOICE Performance	27
4.9	GBR_GAMING Performance	28
4.10	GBR_NON_CONV_VID Performance	28
4.11	NGBR_VID_TCP Performance	28
4.12	No Fading System Parameters	30
4.13	NGBR_VID_VOICE_GAME Performance With Fading	31
4.14	GBR_CONV_VOICE Performance With Fading	31
4.15	GBR_GAMING Performance With Fading	31
4.16	GBR_NON_CONV_VID Performance With Fading	32
4.17	NGBR_VID_TCP Performance With Fading	32

Acronyms

3GPP

3rd Generation Partnership Project

AMC

Adaptive Modulation and Coding

CBRS

Citizens Broadband Radio Service

CQI

Channel Quality Indicator

CTS

Clear to Send

DSA

Dynamic Spectrum Access

eNB

eNodeB

EPC

Evolved Packet Core

FCC

Federal Communications Commission

GAA

General Authorized Access

GBR

Guaranteed Bit Rate

HOL

Head-of-Line

IP

Internet Protocol

ITU-R

International Telecommunication Union Radiocommunication Sector

LTE

Long Term Extension

LTE-U

Long Term Extension - Unlicensed

MAC

Medium Access Control

MCS

Modulation and Coding Scheme

NGBR

Non-Guaranteed Bit Rate

ODFM

Orthogonal Frequency-Division Multiplexing

PAL

Priority Access Licensee

PGW

Packet Data Network Gateway

QAM

Quadrature Amplitude Modulation

QoS

Quality of Service

QPSK

Quadrature Phase Shift Keying

RB

Resource Block

RBG

Resource Block Group

RCQI

Relative Channel Quality Index

RTS

Request to Send

SGW

Serving Gateway

TTI

Transmission Time Interval

UDP

User Datagram Protocol

UE

User Equipment

U.S.

United States

Chapter 1

Introduction

1.1 Introduction

The number of users of wireless radio technologies has greatly increased in the past few years. This has led to an evolving use of the radio spectrum. Currently, all radio bands are allocated by the FCC for specific purposes. This leads to high usage of some spectrum bands and low usage of others. Studies found that up to 82.6% of the spectrum was unused [3]. Most of this spectrum is inaccessible to common users, however it does present the idea that commonly used frequency bands may be inefficiently used. One strategy to use the spectrum more effectively is sharing through Dynamic Spectrum Access (DSA). This is a technique used in the cognitive radio paradigm [4] in which a secondary network is established in the same physical area and frequency band as the primary network. The secondary users will sense the spectrum for holes, then either transmit on open frequencies in open time periods or transmit at a power that will not interfere with other users. These techniques are called interweave and underlay, respectively. In addition to DSA techniques to more efficiently use the spectrum, the regulatory body controlling spectrum allocation in the U.S. has noticed the increased need for bandwidth and has opened the CBRS band of frequencies (3550-3700MHz) to general users. The general users must respect the previous users of the band, called incumbents, and users that purchase licenses,

PAL. The primary incumbent users of the CBRS band are naval radars and satellites.

In addition to the increasing number of people using wireless devices, it should be noted that a 40% of the population lives on the coast in the United States, even though this area only accounts for less than 10% of the nations land mass [5]. This means that many people fall within the exclusion zone that is recommended by regulatory bodies to protect the functionality of the radar [6]. This provides an opportunity for spectrum access if the exclusion distance can be reduced or circumvented through DSA. The close proximity to the coast is notable because it is where naval radars are usually located.

The unused spectrum and the majority of the population being located close to the coast is motivation to closely study dynamic spectrum access near the coast. This may include avoiding naval radar. Naval radar can be modelled as a periodic signal with a peak in signal every rotation [7].

The contribution of this paper is to present a radar aware scheduling algorithm.

1.2 Background

Over the past few years, usage of the radio spectrum has become an increasingly important concern. More users than ever are using wireless technologies in their everyday lives including cellular phones, Bluetooth devices and smart home devices. This is putting a strain on the limited radio bandwidth that consumers can use. Those in charge of spectrum allocation have noticed and have started adapting how the spectrum is used and who can use it. Some bands that are opening will allow general access, but only if the new devices do not interfere with the incumbent users of the frequency. One such band is the CBRS band [8]. This consists of frequencies from 3550 MHz to 3700 MHz, which is unique in pioneering a model for spectrum sharing. In this band there are three tiers of users, incumbents, which includes the U.S. Navy, Priority Access Licensees (PAL) and General Authorized Access (GAA)

users. The incumbents must not be interfered with. PAL users must not be interfered with by GAA users. GAA users must not interfere with anyone. The primary incumbent user of the CBRS band is the U.S. Military for radars, satellite providers and communication. The U.S. population is most dense in port cities near the coast, which is primarily where radar technologies are used. Some studies have been done attempting opportunistic transmission in the presence of radar.

The NS-3 discrete network simulator was used to simulate the network environment. This provides models of packet switched networks. In NS-3, all devices are nodes. Protocol stacks and applications are then applied to nodes. Applications are tasks that each nodes completes. The simulator connects devices over an abstract channel. The channel can be a physical link or a wireless channel. A wireless channel is used in our simulations. NS-3 has an LTE module that uses the LTE-Evolved Packet Core (EPC) implementation. The module has been partially designed to support the evaluation of DSA. The modelling can take many factors into account such as fading and propagation.

The LTE module is able to track the allocation of individual RBs. This allows careful tracking to confirm that no eNB will transmit when it is under the radar beam. In addition, the simulator is able to handle many eNB and even more UE. This allows a realistic simulation with many different devices. The LTE module has abstracted each of the layers used in the LTE protocol stack. A diagram of the LTE stack for the eNB is shown in Figure 1.1.

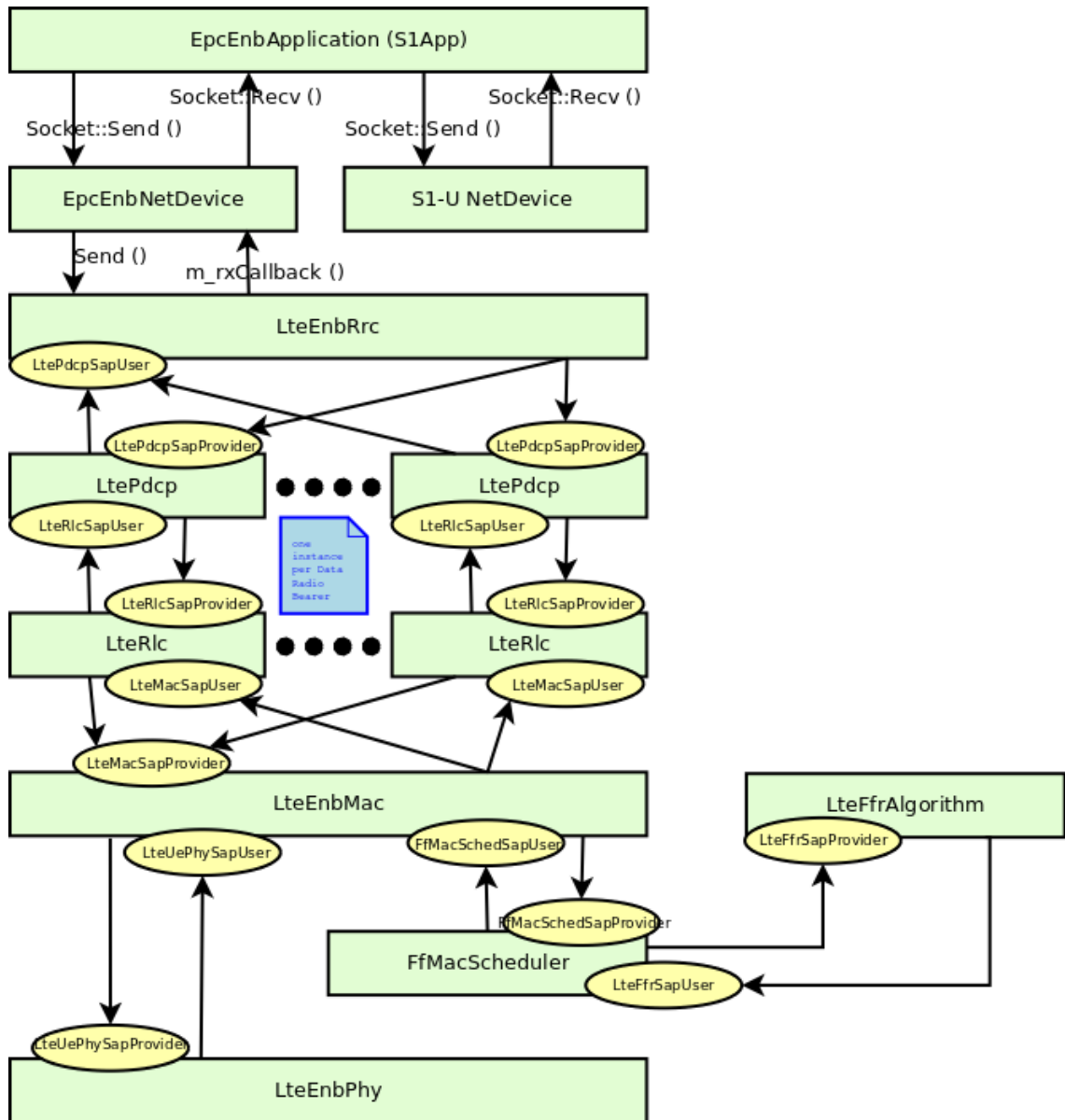


Figure 1.1: NS-3 LTE Radio Protocol Stack for eNodeB

The abstraction of each layer allows scheduling algorithms to be quickly switched and tested. Traffic that flows from S1-U Devices is able to be kept the same between experiments. In addition, lower layers such as the physical layers also remain the same. This system allows for just the performance of the scheduling algorithm to be tested.

The NS-3 module is able to model Adaptive Modulation and Coding (AMC). This

is a process that adjusts the modulation scheme based on channel quality. Periodically, the eNodeB (eNB), a LTE base station, sends a reference signal to the User Equipment (UE), LTE users. Based on the spectral efficiency observed by the User Equip, a Channel Quality Indicator (CQI) is reported. The CQI is standardized by the 3GPP in [1]. The table that the UE uses to determine CQI is shown in Figure 1.2.

CQI index	modulation	code rate x 1024	efficiency
0	out of range		
1	QPSK	78	0.1523
2	QPSK	120	0.2344
3	QPSK	193	0.3770
4	QPSK	308	0.6016
5	QPSK	449	0.8770
6	QPSK	602	1.1758
7	16QAM	378	1.4766
8	16QAM	490	1.9141
9	16QAM	616	2.4063
10	64QAM	466	2.7305
11	64QAM	567	3.3223
12	64QAM	666	3.9023
13	64QAM	772	4.5234
14	64QAM	873	5.1152
15	64QAM	948	5.5547

Figure 1.2: Reprinted from 3GPP TS 36.213 [1]

The higher the efficiency and CQI Index, the higher code rate achievable. There are three modulation schemes supported by NS-3, Quadrature Phase Shift Keying (QPSK), 16-quadrature amplitude modulation (16-QAM), and 64-QAM. Modulation schemes such as 64-QAM support a higher data rates, but are more vulnerable to interference. The CQI and spectrum efficiency are then used to calculate the MCS. MCS is an estimation and not exact. There are 28 MCS classes which are used to calculate which modulation scheme will be used and the size of the transport block. The transport block is how much data can be effectively transmitted in each resource block (RB). The RB is a 1ms/180kHz block of time and frequency [9]. This is the most basic unit in orthogonal frequency-division multiplexing (ODFM) system used in LTE.

Scheduling is another factor that must be taken into account. Recently, many

studies have been performed that optimize how each RB is used. This approach is possible to apply to the CBRS band even though most current implementations of LTE use a lesser frequency, some companies are using LTE-U in this band [10].

The first scheduling algorithm that will be leveraged is the proportional fair algorithm as explained by [11]. This algorithm schedules a user when the current channel quality is high compared to its past quality. In order to calculate this, the algorithm uses the current achievable rate divided by the past averaged throughput to calculate a relative channel quality indicator (RCQI). In the NS-3 simulator LTE module [2] the proportional fair algorithm works as follows. Let i, j be generic users; t be the subframe index; k be the resource block index; $M_{i,k}(t)$ be the MCS of user i at RB k and $S(M, B)$ be the transport block size when B blocks are used. The achievable rate is calculated by Equation 1.1.

$$R_i(k, t) = \frac{S(M_{i,k}(t), 1)}{\tau} \quad (1.1)$$

This calculates the achievable rate for one user, i , using RB k in subframe t . τ is the duration of one TTI, which is 1ms in LTE. After the achievable rate is calculated, it is used in Equation 1.2 to allocate each RBG.

$$\hat{i}_k(t) = \operatorname{argmax}_{j=1, \dots, N} \left(\frac{R_j(k, t)}{T_j(t)} \right) \quad (1.2)$$

$T_j(t)$ is the past throughput for user j . This establishes the RCQI as indicated earlier. The UE with the best RCQI is allocated the RBG. The past throughput for user j is shown in Equation 1.3.

$$T_j(t) = \left(1 - \frac{1}{\alpha}\right) * T_j(t-1) + \frac{1}{\alpha} * \hat{T}_j(t) \quad (1.3)$$

The past average throughput is calculated using the exponential moving average approach. $\hat{T}_j(t)$ is the throughput achieved by the user j in the subframe t . The

process to calculate $T_j^{\hat{}}(t)$ is as follows. First the MCS is determined using Equation 1.4.

$$\hat{M}_j(t) = \min_{k:\hat{i}_k(t)=j} M_{j,k}(t) \quad (1.4)$$

The minimum supported MCS is used. This gives the best throughput to error rate. The total number of RBGs allocated to the user is then counted based on the number of RBGs and when user j had the highest RCQI. The throughput for the subframe, $\hat{T}_j(t)$ is then calculated using Equation 1.5.

$$\hat{T}_j(t) = \frac{S(\hat{M}_j(t), \hat{B}_j(t))}{\tau} \quad (1.5)$$

This is the process for the proportional fair algorithm. This algorithm was fully implemented within the NS-3 simulator [2]. A delay aware proportional fair algorithm was created that changed the $\hat{i}_k(t)$ to the equation shown in Equation 1.6.

$$\hat{i}_k(t) = \operatorname{argmax}_{j=1,\dots,N} \left(\exp \left[\frac{w_{i,j}(t) - T_j}{T_j} + \frac{R_j(k,t)}{T_j(t)} \right] \right) \quad (1.6)$$

This added a delay aware aspect to the proportionally fair algorithm. The usual proportionally fair algorithm does not have any QoS delay awareness.

The rest of this paper is organized as follows. Chapter II describes the system setup. The radar aware scheduling algorithm is outlined in Chapter III. Simulation results are presented in Chapter IV, followed by conclusions in Chapter V.

1.3 Previous Work

Many recent works have focused on DSA in the CBRS band. The most notable to this thesis is [12]. This studies the feasibility of coexistence of LTE-U with a rotating radar in the CBRS band. The authors found that it is possible for an LTE-U eNodeB

to coexist with radar, however, if the naval radar had a high gain, the signal to noise ratio for the down-link radio would severely deteriorate. In addition, the authors showed a basic way to model a rotating radar. Although practically, radar is not perfectly periodic, it can be modelled as such for the purpose of analysis. A model for beam directivity ($G(\theta)$) is given in [12], based off of ITU-R recommendations [7].

The given formula is

$$G(\theta) = \begin{cases} \frac{\pi}{2} \left(\frac{\cos(68.8\pi \sin(\theta))}{(\frac{\pi}{2})^2 - (\frac{68.8\pi \sin(\theta)}{\theta_{3dB}})^2} \right), & -10^\circ \leq \theta \leq 10^\circ \\ -60 \text{ dB}, & \text{otherwise} \end{cases}$$

θ_{3dB} is the half power beamwidth of the antenna. A common half power beamwidth for naval radar is 0.81° . The radar antenna pattern can then be modelled over time.

This is shown in Figure 1.3.

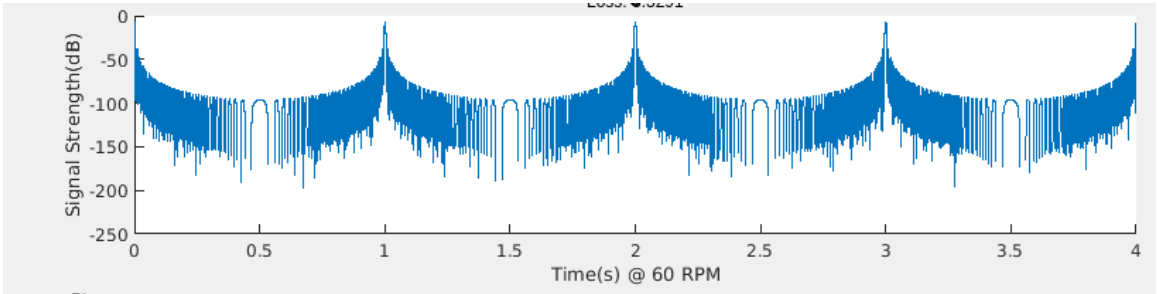


Figure 1.3: Radar Beam Pattern at 60 RPM

This beam model is able to be used to determine when the radar transmission is at a maximum at a node. This is based on standards from regulatory bodies such as the ITU-R [7] and the U.S. Department of Commerce [6].

Other papers focused on multi-user transmission. This is a common issue for any multiple-user, decentralized network. A Medium Access Protocol (MAC) protocol such as one proposed in [13] may be helpful. This uses Request-to-send (RTS) and Clear-to-send (CTS) messages, similar to what is done in Wi-Fi. In addition, a cognitive model is applied that maximizes when RTS and CTS messages are sent. The radar beam can be taken into account for when RTS messages are sent, as

knowledge of the periodic signal will be known and the round trip time for sending RTS and receiving the CTS message will also be known.

Another paper [14], studied adaptive scheduling. This algorithm places a priority on each type of traffic based on desired quality-of-service (QoS). There are three important pieces of the priority function, the k term, which prioritizes real time traffic when the number of available RBs shrinks, the α term takes into account the guaranteed delay against the current observed delay and the β term takes into account the current throughput against the expected throughput. The equation for the priority function is shown in Equation 1.7.

$$p(i, j) = k_j * \exp[\alpha_j * \frac{w_{i,j}(t) - T_j}{T_j} + \beta_j * \frac{r_j - \bar{r}_{i,j}}{r_j}] \quad (1.7)$$

$p(i, j)$ is the priority of queue j of user i . i is a generic user. j is a generic traffic stream. α_j and β_j are weights to balance delay vs throughput priority. Their sum should be 1. T_j is the maximum packet delay. r_j is the expected packet throughput. $w_{i,j}(t)$ is the current observed delay of the Head-of-line (HOL) packet. $\bar{r}_{i,j}$ is the average throughput of traffic queue j of user i . k_j is the real time adaptive coefficient. k_j is calculated using Equation 1.8.

$$k_j = \begin{cases} 1 + \frac{u(N-\bar{N})}{N}, & \text{Traffic class } j \text{ is real-time} \\ 1, & \text{Traffic class } j \text{ is non-real-time} \end{cases} \quad (1.8)$$

N is the mean number of available subchannels and \bar{N} is the number of subchannels currently available. $u()$ is the unit-step function. Using k_j places a higher priority on real-time traffic when available channels decrease. This will be helpful in providing a QoS based scheduling algorithm. Many of the other algorithms only take the channel quality into effect or are not adaptive. In addition, many scheduling algorithms are not aware of QoS requirements.

1.4 Motivation

The motivation for this work is to more efficiently use the radio spectrum in the coastal areas. This is an area with a high population density and will require a more optimally used spectrum to service an increasing number of user's data needs. End users will be able to take advantage of the higher throughput to support applications such as video streaming and browsing social media.

1.5 Novel Contribution

The new idea present is a periodically changing scheduler. Based on the rotation of the radar, the availability of the transmitter and routes will change. The scheduling algorithm will detect when the radar beam is overhead and know when the transmitter is able to transmit. It is assumed that the radar is perfectly periodic.

The scheduling algorithm does not just mute transmission, it uses the amount of time transmission will be muted due to the radar, the current channel conditions and QoS requirements in order to maintain the required QoS most efficiently. This allows users to experience the QoS that is expected and does not interfere with the incumbent radar. By using real-time channel quality measurements, the base station can maximize overall throughput in addition to maintaining QoS requirements.

Chapter 2

System Setup

Using the NS-3 simulator, a simulation environment was created. This simulator allows the entire LTE stack and Internet Protocol (IP) to be simulated and takes a variety of factors into account including physical layout, fading, and Adaptive Modulation and Coding (AMC). In the simulated system, there were five UE and one eNB. This was used for all of the simulations. Simulations were run until the queue length reached a steady state.

2.1 Physical Layout

For the simulations, an eNB was placed, then five UE placed in a uniform disc around the eNB. The distance between could be adjusted to vary the effects of fading and propagation loss on the signal. Figure 2.1 shows the physical layout of the setup.

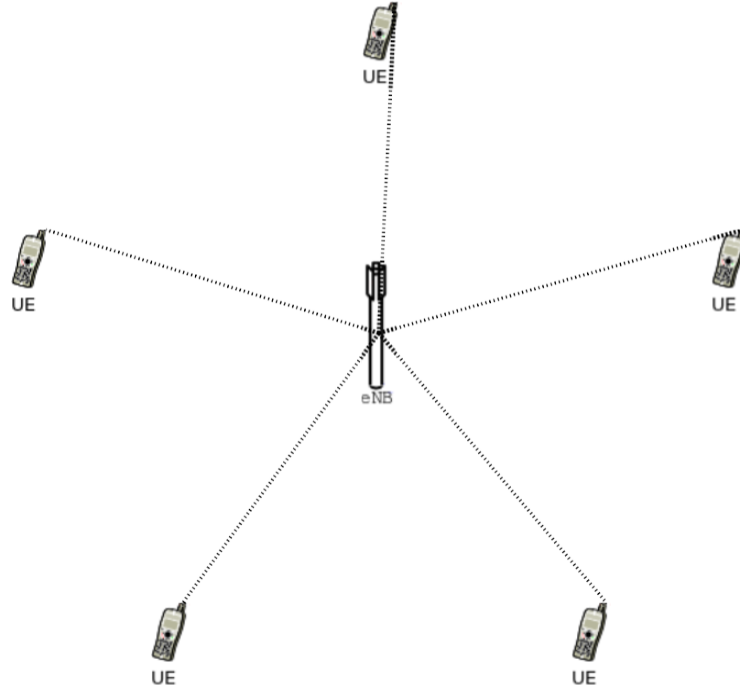


Figure 2.1: User Equipment and EnodeB Layout

This layout keeps the propagation loss the same for all of the UE. Signal degradation due to fading will be different. While each UE experiences different fading, it is constant between each run, so that the channel conditions are consistent when different scheduling algorithms are tested.

2.2 Channel Characteristics

Signal degradation was simulated. Propagation loss and fading were able to be simulated. Some experiments were run without fading. The Friis Model was used as

outlined in [15] for both path loss and fading. Simulating these increases how realistic the channel is modelled.

In addition, the adaptive modulation and coding system that was mentioned in Section 1.2 was used. This changes the size of the transport block based on the channel condition from fading and propagation loss. This is a realistic system that is used that varies the throughput that a channel can experience.

2.3 LTE and Internet Protocol

In the simulation, the IP stack was installed on the eNB and UE. In order to simulate traffic, an external device connected through the internet sent User Datagram Protocol (UDP) traffic to each UE. The network topology is shown in Figure 2.2.

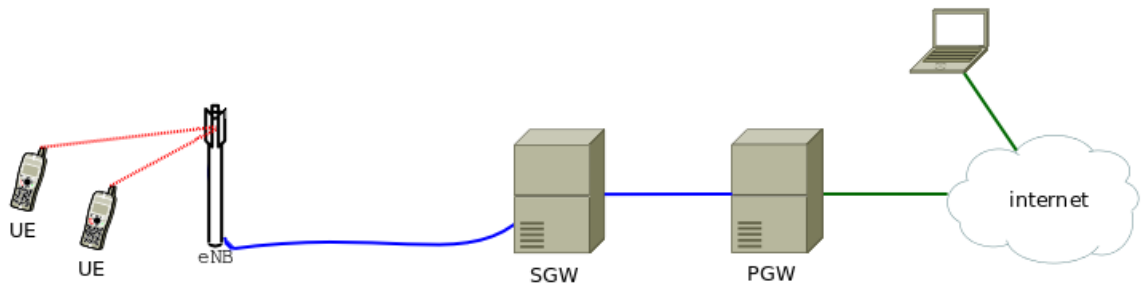


Figure 2.2: Network Topology of Simulated Network

The Packet Data Network Gateway (PGW) and Serving Gateway (SGW) are nodes that are part of the Evolved Packet Core (EPC). This is part of the LTE model. The PGW provides access to the internet and other services to down-link users. The SGW receives and forwards packets from the PGW to the correct eNB. The SGW also keeps track of IP bearer services. The Evolved Packet System (EPS) as outlined in [16] maintains QoS for the UE.

The EPS bearer uses QoS Class Identifiers (QCI) to ensure traffic QoS requirements are upheld. This signals to the eNB what type of traffic is being transmitted. This is used to keep traffic under delay constraints and under packet error loss rates.

There were five different traffic classes used in simulation. These are shown with their QCI identifier, resource type, delay budget and example services in Table 2.1.

QCI	Resource Type	Max Delay	Example Services
1	GBR	100ms	Conversational Voice
3	GBR	50ms	Real Time Gaming
4	GBR	300ms	Non-Conversational Video
7	Non-GBR	100ms	Video (Live Streaming), Interactive Gaming
9	Non-GBR	300ms	TCP-Based Buffered Video Streaming

Table 2.1: QCI Information Used in Simulation

The resource type is if the traffic has a guaranteed bit rate or not. Guaranteed bit rate traffic has a bandwidth that is guaranteed. There are many other QCI indicators outlined in [16], but only five were used in the simulation.

2.4 Radar Modelling

In the simulations, a simple model was used for the radar. The model from the ITU-R [7] and shown in [12] was used. The pattern is shown in 1.3. An experiment was conducted using Matlab. Using the previously mentioned model, observation of the radar was done at different points. The observed peak of the radar is different based on location. Examples of this are shown in Figure 2.3.

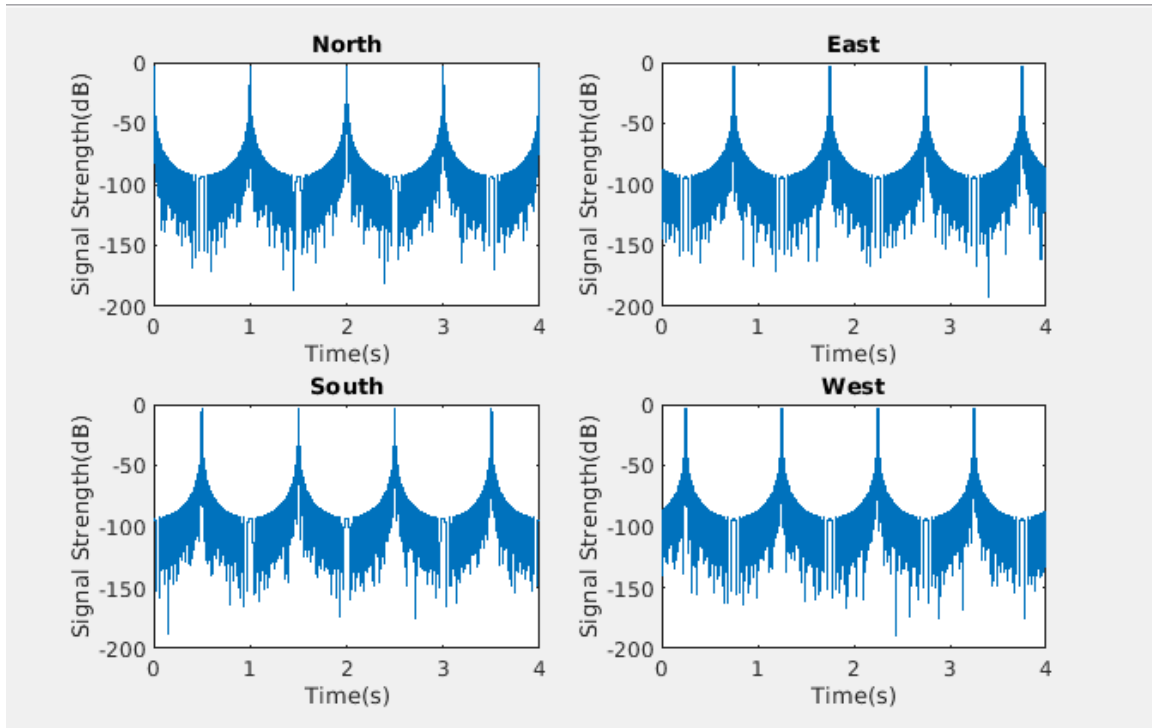


Figure 2.3: Radar Beam Observed at Different Locations

The observed peak is shifted at each location. This is a very simple model of the radar, but is sufficient. Four distinct locations were shown, but there are many more possible. An interactive program was created in Matlab that allowed the user to move a point around a circle and the observed radar beam would be shown.

Chapter 3

Radar-Aware Transmission and Scheduling

3.1 Radar-Aware Transmission and Scheduling

The scheduling algorithm is different from classic schedulers in that it is able to dynamically change based on channel conditions and in our case based on the radar. The proposed algorithm uses the current HOL delay of the queues and the current channel conditions to provide timely transmission of packets. In addition, the proposed algorithm puts a priority on GBR traffic, to minimize the radar effects on guaranteed traffic. The algorithm is also aware of when each UE will experience the effect of the radar and boosts transmission such that the overall delay experienced will be minimized.

In order to create this algorithm, the proportional fair algorithm was studied. This provided a good starting point that balanced all of the traffic. Packets are scheduled based on their relative channel quality and past throughput. When there are no differentiating factors between UE, all of the traffics will have the same average throughput. Next, a boost period was added. This is for all traffic classes and provides a temporary boost to each stream by adding the upcoming delay onto the traffic queue length. This prioritizes the traffic that is about to be muted due to the radar beam. Next, a delay aware aspect was added to the algorithm. This was adapted from the adaptive scheduling algorithm in [14]. The priority equation shown in Equation 1.7

was changed and merged with the proportional fair algorithm. The α term focuses on the delay and the β term is the proportional fair aspect. The sum of the α and β terms is one. The terms can be changed to place a higher weight on the delay aspect or the proportional fair aspect of scheduling. Another part of [14] that was adapted was the k term becoming the p term. In the previous adaptive algorithm, the k term added a higher priority to real-time traffic when the amount of available subchannels dropped below the mean available amount of subchannels. In the proposed situation, the number of available subchannels is more consistent, but when the radios can transmit is changing. The adaptation has been made to change the k , which is in the frequency domain, to the p term, which is the time domain. The p term becomes active when there is less than the mean time remaining until the radar beam causes the radio to mute. This allows GBR traffic to more likely meet QoS requirements. All of the equations used in the calculation are shown below.

First, the achievable rate is calculated the same as the proportional fair algorithm as shown in Equation 1.1. Let i be a generic user and j be a flow of user i . The algorithm then allocates RBGs to active users using Equation 3.1.

$$\hat{i}_k = \operatorname{argmax}_{j=1, \dots, N} \begin{cases} 0, & t_{j,off} < t < t_{j,on} \\ p_j * \exp[\alpha_j * \frac{w_{i,j}(t) - T_j}{T_j} + \beta_j * \frac{R_j(k,t)}{T_j(t)}] & , \text{ otherwise} \end{cases} \quad (3.1)$$

$t_{j,off}$ is the time when flow j must be muted as to not interfere with the radar. $t_{j,on}$ is when the flow j is able to resume transmission. α_j and β_j are weights that change how much weight is placed on the delay awareness or the channel awareness. Their sum is 1. T_j is the maximum allowed delay as required from QCI. $R_j(k, t)$ is the achievable rate for the stream j in the current RB. $T_j(t)$ is the exponential moving average throughput of the stream j as calculated in Equation 1.3. p_j is the priority of the stream j . $w_{i,j}(t)$ is the queue delay experienced by stream j for user i , in addition to a boost in performance when the radar is approaching. This is calculated using

Equation 3.2.

$$w_{i,j}(t) = \frac{Q_{i,j}(t)}{R_j(k, t)} + u(t - t_{j,off} + \Delta t_j) * 1.5\Delta t_j \quad (3.2)$$

In this equation, $Q_{i,j}(t)$ is the length of the queue of stream j . $u(\cdot)$ is the unit-step function. Δt_j is the amount of time that the radio is muted to not interfere with the radar. By accounting for the delay due to the radar, peaks in queue delay are able to be minimized. Another part that helps minimize queue delay for GBR traffic is the priority term p_j . The equation for this is shown in Equation 3.3.

$$p_j = \begin{cases} 1 + \frac{u(t_{avg} - t_{remaining})}{t_{avg} * 2}, & \text{GBR Traffic} \\ 1, & \text{Non-GBR Traffic} \end{cases} \quad (3.3)$$

In this equation, t_{avg} is the average time remaining before the transmitter is required to mute and $t_{remaining}$ is the amount of time remaining before the transmitter is required to mute. As the time approaches that the radio must mute transmissions, the p_j term increases, putting a higher priority on GBR traffic. After the RBGs are allocated, the remaining steps in the proportional fair algorithm are followed including calculating the proper MCS as shown in Equation 1.4 and the actual throughput for the user i in subframe at t as shown in 1.5.

The algorithm prioritizes GBR traffic, minimizes the effect of muting for the radar of packet delay and maintains delay requirements according to QCI.

Chapter 4

Results

There were two main simulation scenarios that were run, with fading and without fading. Three algorithms are compared, the proportional fair, as outlined in [11] and Section 1.2, proportional fair with delay awareness, as outlined in Section 1.2 and the proposed algorithm, as outlined in Chapter 3.1. For each of these the α_j and β_j terms were adjusted. The α_j term determines how much weight is placed on the queue delay and the β_j term weights how much the scheduler will perform like the proportional fair.

4.1 Experimental Setup

4.1.1 NS-3 Setup

The simulator used was the NS-3 simulator. This simulates all of the discrete events within Internet Systems [2]. This is organized in such a way that user modules can be created and all source code is available to edit. Each part of the network is broken into modules and most have classes that assist the user with setup and customization. In addition, there are plenty of examples to help new users get started. The NS-3 simulator allows simulation of the LTE-EPC stack and allows for IP connectivity with only a few lines of code for setup. The IP stack can be used between two devices easily without the user having to worry about implementing their functionality. Figure 4.1

shows how this is implemented.

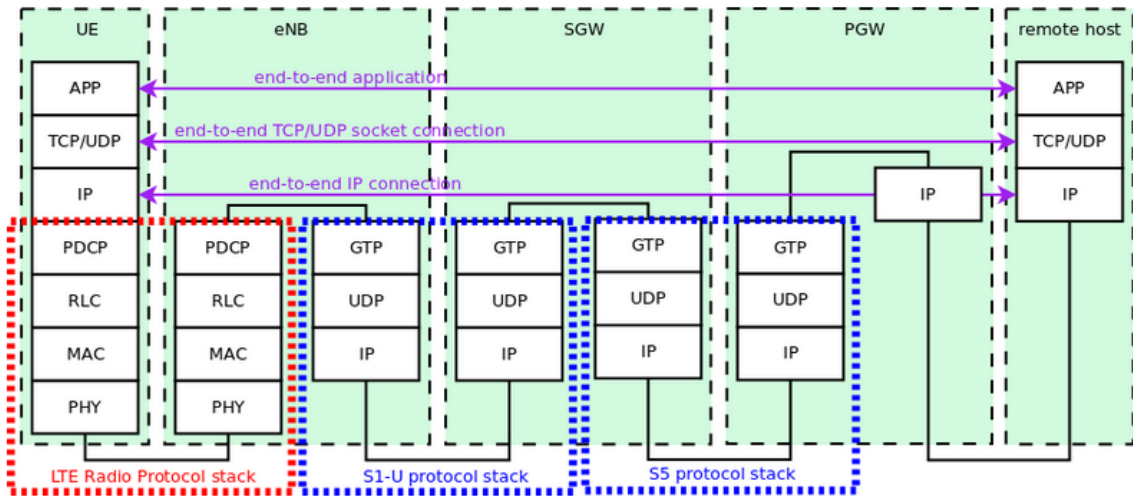


Figure 4.1: LTE-EPC Stack in NS-3 [2]

Each of the blocks are different parts of the LTE-EPC stack and can be modified. For the experiment, the MAC layer of the eNB was modified to implement the proposed algorithm and the other algorithms that were used for comparison. A new module was added to MAC layer. The downlink scheduling function was modified to determine the results. In NS-3 this function is called `DoSchedDITriggerReq`. The changes that were made to implement the proposed algorithm were assigning each stream an offset of when they would be required to turn off, adding awareness of turning off to the scheduling function and implementing the proposed algorithm to select which UE will get allocated each RB.

4.1.2 Design of Experiments

For the experiments, a variety of traffic classes were present. These included both GBR and NGBR traffic. Also, traffic with different delay constraints were selected. Traffic was also selected to reflect real use of a network with different services. Classes that support services such as buffered video streaming, live-streaming video, online gaming and conversational voice were used. Another change that was made for each of

the simulations was the packet size. This was determined by using different values and increasing until the system reached a steady state without all traffic classes meeting their QoS requirements all of the time. If the packet size decreased then all traffic would meet their requirements and the comparison would be more difficult to observe. If the packet size is decreased too much, then all traffic classes will perform similarly, as there is not enough traffic to load the network.

In order to determine which α_j and β_j terms performed the best, simulations were run that changed each of the weights by 0.05. These were repeated until a good balance between the GBR and NGBR traffic was reached. The goal is to minimize the amount of time that the traffic is above the delay constraint. Once a good balance was reached, the traffic was changed by 0.01 to find the most optimal. There were multiple ratios that performed favorably.

4.2 No Fading Results

The partial simulation parameters are shown in Table 4.1 below.

Parameter	Value
Packet Size	2160 Bytes
Packet Arrival Rate	200 / s
Delay Due to Radar	50 ms
GBR α_j value	0.4
GBR β_j value	0.6
NGBR α_j value	0.6
NGBR β_j value	0.4
UE Distance from ENb	100m
θ_{3dB} of Radar	0.81°
Radar Rotation Speed	60 rpm

Table 4.1: No Fading System Parameters

The parameters for α_j and β_j were found by varying the values and finding which resulted in the best performance. Many experiments were run with small changes to the α_j and β_j terms. The results were then recorded against each other and the result that had the best relative performance between the GBR and NGBR was selected. The results for the simulation without fading are shown in the Tables below.

NGBR_VID_VOICE_GAME	Maximum QoS Delay: 100ms			
	Mean Delay (ms)	Standard Deviation (ms)	Maximum Delay (ms)	Probability Over
Proposed Algorithm	92.1	15.9	162.0	0.221
Proportional Fair	12.6	11.2	93.7	0
Proportional Fair + Delay Awareness	91.9	21.8	230.4	0.208

Table 4.2: NGBR_VID_VOICE_GAME Performance Without Fading

GBR_CONV_VOICE			Maximum QoS Delay: 100ms	
	Mean Delay (ms)	Standard Deviation (ms)	Maximum Delay (ms)	Probability Over
Proposed Algorithm	76.9	18.4	116.4	0.045
Proportional Fair	11.9	7.8	54.8	0
Proportional Fair + Delay Awareness	85.6	20.7	143.3	0.153

Table 4.3: GBR_CONV_VOICE Performance Without Fading

GBR_GAMING			Maximum QoS Delay: 50ms	
	Mean Delay (ms)	Standard Deviation (ms)	Maximum Delay (ms)	Probability Over
Proposed Algorithm	34.4	13.4	69.1	0.046
Proportional Fair	12.7	7.6	55.0	0.004
Proportional Fair + Delay Awareness	40.4	16.8	104.5	0.160

Table 4.4: GBR_GAMING Performance Without Fading

GBR_NON_CONV_VID			Maximum QoS Delay: 300ms	
	Mean Delay (ms)	Standard Deviation (ms)	Maximum Delay (ms)	Probability Over
Proposed Algorithm	255.9	41.4	384.9	0.159
Proportional Fair	13.5	7.9	54.6	0
Proportional Fair + Delay Awareness	283.6	43.7	516.3	0.260

Table 4.5: GBR_NON_CONV_VID Performance Without Fading

NGBR_VID_TCP			Maximum QoS Delay: 300ms	
	Mean Delay (ms)	Standard Deviation (ms)	Maximum Delay (ms)	Probability Over
Proposed Algorithm	276.7	31.7	460.3	0.146
Proportional Fair	11.7	7.2	51.9	0
Proportional Fair + Delay Awareness	258.6	41.8	515.2	0.092

Table 4.6: NGBR_VID_TCP Performance Without Fading

In this case, the proportional fair algorithm was able to outperform the others, as it was not concerned with the delays and there was enough bandwidth that allowed all users to stay under their delay constraints. The effects of the p , α and β terms were able to be seen. These are reflected in a lower Mean Delay (ms) for the gaming traffic in the proposed algorithm, compared to the proportional fair with delay awareness. The radar-aware aspect of the proposed algorithm was able to minimize

the max delay which caused all traffic classes had a lower maximum delay than the proportional fair + delay awareness. Histograms were also created that showed the distribution of queue delay throughout the simulation. The histogram for proportional fair simulation is shown in Figure 4.2.

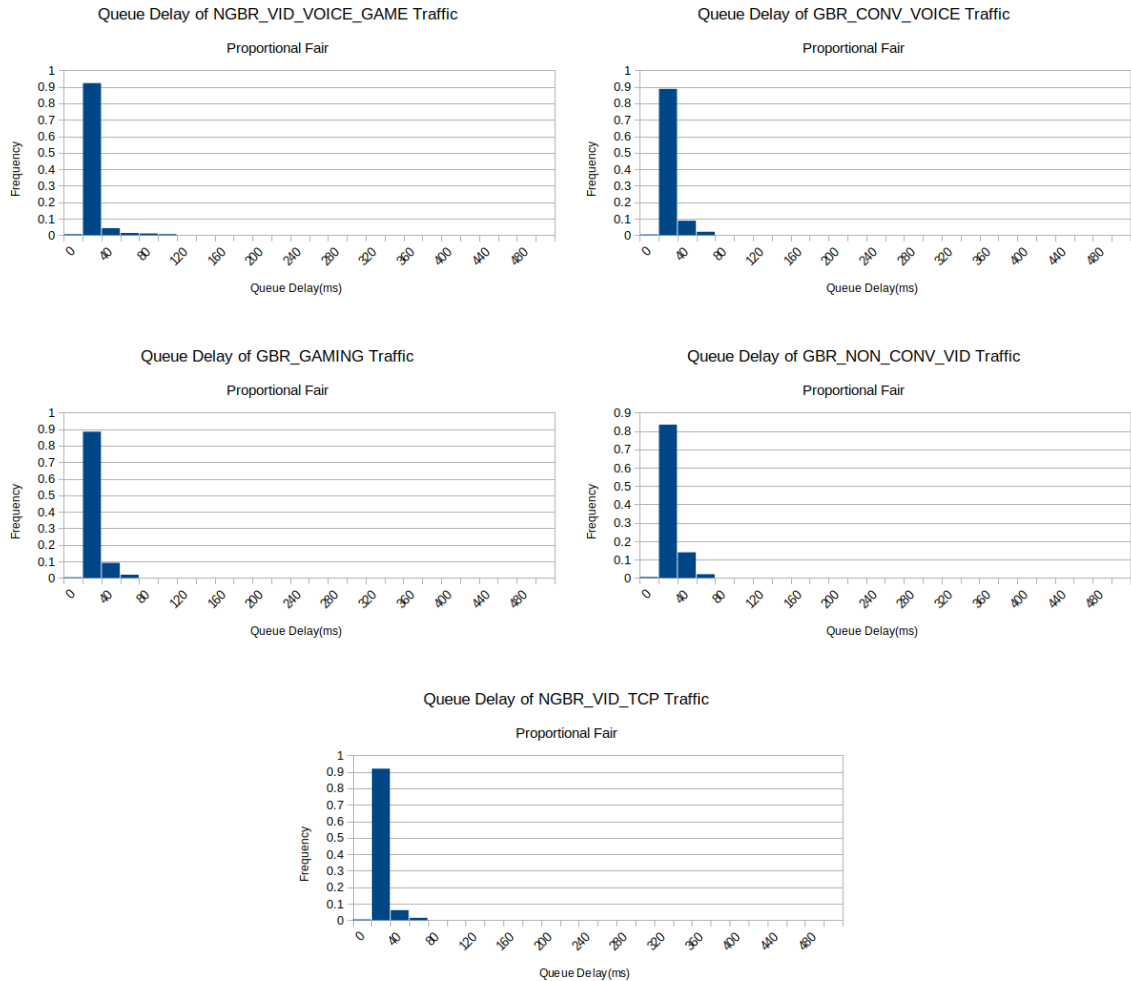


Figure 4.2: Histograms of Proportional Fair No Fading

As expected, all of the traffic has a very similar distribution. Proportional fair keeps the throughput of the streams equal. This is because all of the channels have the same channel conditions. There is no difference to how the proportional fair scheduler treats the GBR and NGBR traffic. Next, the histogram of the proportional fair with delay awareness is shown in Figure 4.3.

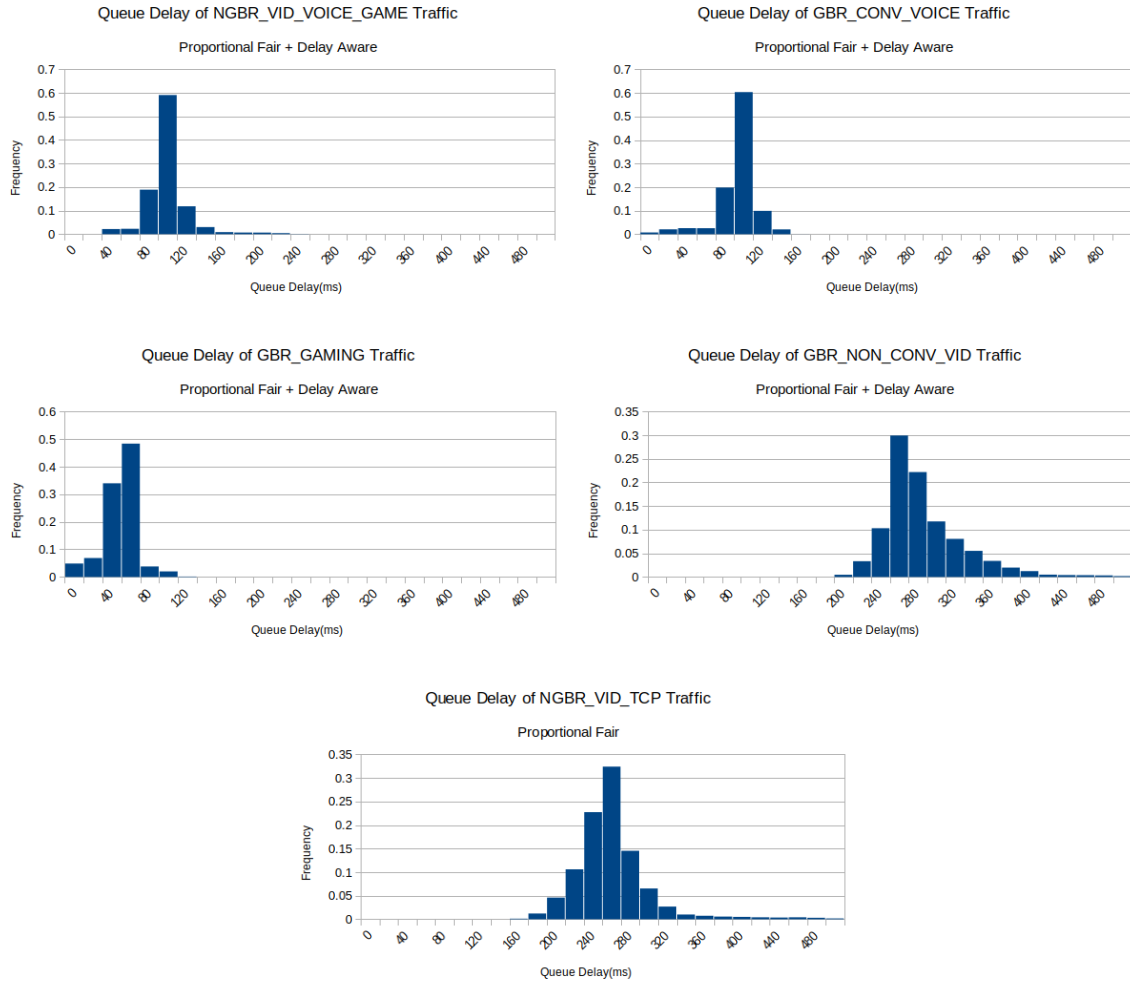


Figure 4.3: Histograms of Proportional Fair Delay Aware No Fading

This algorithm had more spread than the proportional fair due to the delay awareness. The two streams with the highest delay, GBR_NON_CONV_VID and NGBR_VID_TCP were separate from the other three. There is similar performance of the GBR_NON_CONV_VID and NGBR_VID_TCP because both of their delay constraints are 300ms. There are also similarities between the GBR_CONV_VID and NGBR_VID_VOICE_GAME traffic because they have the same delay constraint of 100ms. THE GBR_GAMING traffic has many points that are in the first two classes of 20ms and 40ms because the delay constraint is 50ms. This is true for the The histogram of the proposed algorithm is shown in Figure 4.4.

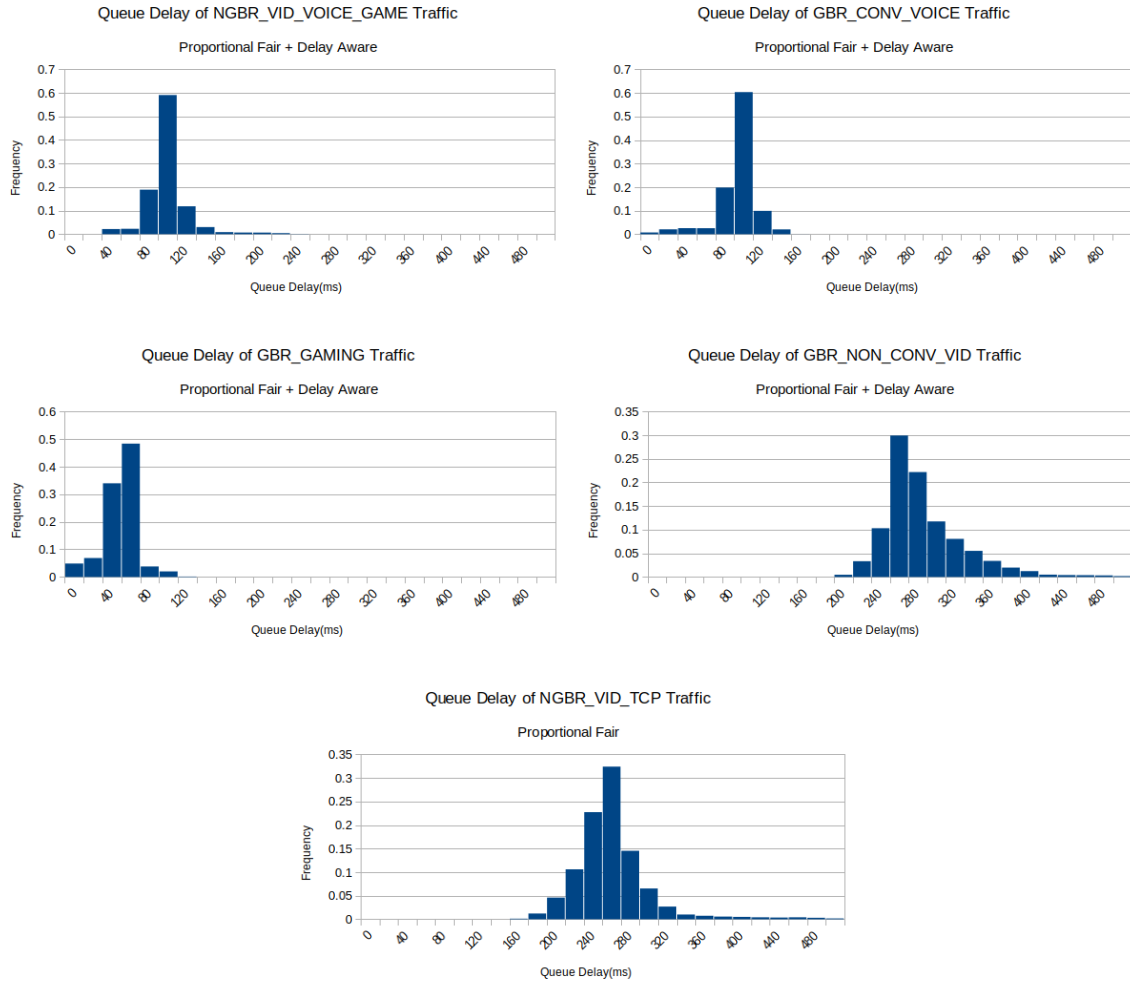


Figure 4.4: Histograms of Proposed Algorithm No Fading Traffic

The proposed algorithm has a wider distribution than the other algorithms, due to the multiple factors that the proposed algorithm takes into account. This allows better performance for the low latency QoS flows. Within these graphs, the tail to the left, prominent in the GBR_CONV_VOICE traffic, is due to the priority that is placed on GBR traffic and the boost period that is present immediately prior to ceasing transmissions for the radar. The tail of the right, easily seen in the NGBR_VID_TCP traffic, is due to the stopping transmissions to not interfere with the radar. There is also some differentiation between the GBR and NGBR traffic with the same delay constraints. This is because the proposed algorithm places a higher priority on the

GBR traffic. Due to overall throughput being a finite resource, the NGBR traffic suffers worse performance.

4.2.1 The Process to Final Values

There were a variety of attempts prior to finding a favorable result. Different values for α_j and β_j were used in addition to using different values in the denominator of the priority function. The tables below shows some of the intermediate steps, along with a reference.

NGBR_VID_VOICE_GAME			Maximum QoS Delay: 100ms	
	Mean Delay (ms)	Standard Deviation (ms)	Maximum Delay (ms)	Probability Over
Reference	92.2	15.6	164.6	0.222
P Value 1/1	103.3	18.2	184.0	0.642
P Value 1/4	83.2	14.7	151.2	0.085
Both Alpha 0.75	94.8	19.4	166.1	0.364
Both Alpha 0.25	113.8	21.0	224.8	0.805
No Radar Delay	95.5	21.5	246.6	0.239

Table 4.7: NGBR_VID_VOICE_GAME Performance

GBR_CONV_VOICE			Maximum QoS Delay: 100ms	
	Mean Delay (ms)	Standard Deviation (ms)	Maximum Delay (ms)	Probability Over
Reference	71.3	18.4	108.5	0.016
P Value 1/1	62.6	22.3	108.9	0.030
P Value 1/4	73.6	16.3	122.7	0.022
Both Alpha 0.75	73.6	18.5	121.2	0.028
Both Alpha 0.25	55.1	20.5	95.8	0
No Radar Delay	73.6	18.7	118.9	0.024

Table 4.8: GBR_CONV_VOICE Performance

GBR_GAMING			Maximum QoS Delay: 50ms	
	Mean Delay (ms)	Standard Deviation (ms)	Maximum Delay (ms)	Probability Over
Reference	32.1	12.7	65.5	0.030
P Value 1/1	28.7	12.9	55.6	0.058
P Value 1/4	33.0	12.5	73.3	0.037
Both Alpha 0.75	33.0	13.0	66.4	0.034
Both Alpha 0.25	25.4	11.4	51.0	0
No Radar Delay	34.6	14.2	94.1	0.076

Table 4.9: GBR_GAMING Performance

GBR_NON_CONV_VID			Maximum QoS Delay: 300ms	
	Mean Delay (ms)	Standard Deviation (ms)	Maximum Delay (ms)	Probability Over
Reference	237.3	41.7	370.0	0.086
P Value 1/1	211.8	42.3	317.5	0.012
P Value 1/4	242.5	39.0	380.9	0.089
Both Alpha 0.75	245.1	42.6	389.0	0.134
Both Alpha 0.25	193.5	35.0	310.1	0.000
No Radar Delay	239.2	43.1	446.3	0.082

Table 4.10: GBR_NON_CONV_VID Performance

NGBR_VID_TCP			Maximum QoS Delay: 300ms	
	Mean Delay (ms)	Standard Deviation (ms)	Maximum Delay (ms)	Probability Over
Reference	282.0	30.5	468.2	0.153
P Value 1/1	327.8	35.5	529.3	0.818
P Value 1/4	243.7	29.4	408.2	0.037
Both Alpha 0.75	294.0	35.0	487.6	0.348
Both Alpha 0.25	375.7	41.7	611.9	0.996
No Radar Delay	283.8	39.8	571.2	0.156

Table 4.11: NGBR_VID_TCP Performance

The reference is the proposed algorithm as is. The P value 1/1 places a much higher priority on the GBR traffic, at the cost of the NGBR traffic. This changes the denominator of the P function shown in Equation 3.3. This change removed the factor

of two. The P value $1/4$ changed the factor in the denominator to 4. This placed too little priority on the GBR traffic, which allowed the NGBR traffic to outperform it. Changing both of the α values to 0.75 had no meaningful effect on the result and overall decreased performance. Changing both of the α values to 0.25 allowed the GBR traffic to thrive, but came at a very steep cost to the NGBR traffic. The simulation without radar delay did not artificially increase the length of the queue prior to the transmitter turning off. This led to higher maximum delays and slightly worse performance for the NGBR traffic.

The tables shown above show that a balance is required. If one term is allowed to overpower the others, it will cause one type of traffic to gain too much and the others suffer. The proposed algorithm was able to balance the factors shown above successfully.

4.3 Fading Results

The experiment was then repeated with fading effecting the channel. This reduces the quality of the channel. Algorithms such as the proportional fair do not take into account the queue delay, and thus only maximize the channels that have a good quality. Because of the degradation in channel quality, the achievable throughput decreased. The Friis model [15] was used to simulate the effects of fading. This model is based on the distance the UE are from the eNB The parameters used in the simulation are shown in Table 4.12.

Parameter	Value
Packet Size	1140 Bytes
Packet Arrival Rate	200 / s
Delay Due to Radar	50 ms
GBR α_j value	0.62
GBR β_j value	0.38
NGBR α_j value	0.48
NGBR β_j value	0.52
UE Distance from ENb	10m
θ_{3dB} of Radar	0.81°
Radar Rotation Speed	60 rpm

Table 4.12: No Fading System Parameters

In addition to the throughput decreasing, the distance between the eNB and UE was required to decrease. Radio signals degrade logarithmically and at the previously used distance of 100m, the signal was not strong enough to transmit any data. To determine the α_j and β_j weights for this simulation, the simulation was run with 10 of the possible 120 UE combinations and performance was based off of the average. When a favorable balance was achieved, the simulation was run with all 120 UE combinations and the results were averaged. A histogram of the performance of the proportional fair algorithm is shown in Figure 4.5.

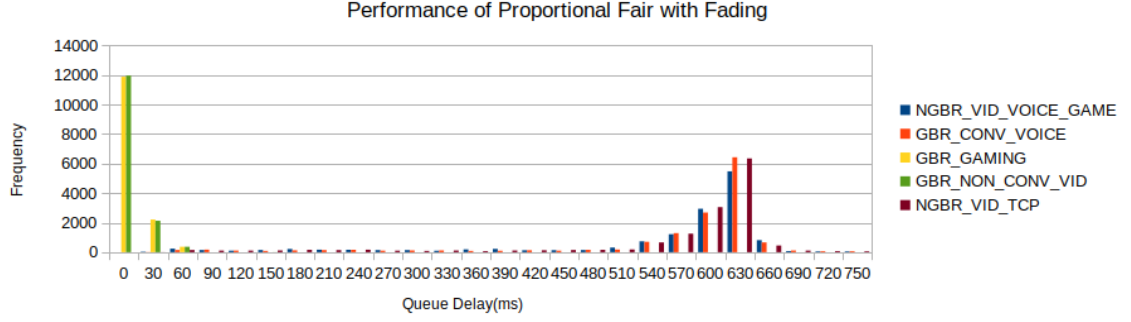


Figure 4.5: Histogram of Proportional Fair Fading

Because the performance is highly related to channel quality, the algorithm prioritized the good channel. This led to neglect of the other traffic and once a steady state was reached, the three streams were all much over their maximum constraints. For this reason, the proportional fair algorithm was excluded from the fading results. The results from the experiment with fading are shown below.

NGBR_VID_VOICE_GAME				Maximum QoS Delay: 100ms
	Mean Delay(ms)	Standard Deviation(ms)	Maximum Delay(ms)	Probability Over
Proposed Algorithm	62.8	19.9	127.1	0.155
Proportional Fair + Delay Awareness	38.0	14.5	103.2	0.063

Table 4.13: NGBR_VID_VOICE_GAME Performance With Fading

GBR_CONV_VOICE				Maximum QoS Delay: 100ms
	Mean Delay(ms)	Standard Deviation(ms)	Maximum Delay(ms)	Probability Over
Proposed Algorithm	38.9	16.1	90.6	0.029
Proportional Fair + Delay Awareness	40.4	14.8	105.8	0.068

Table 4.14: GBR_CONV_VOICE Performance With Fading

GBR_GAMING				Maximum QoS Delay: 50ms
	Mean Delay(ms)	Standard Deviation(ms)	Maximum Delay(ms)	Probability Over
Proposed Algorithm	19.0	10.3	59.4	0.023
Proportional Fair + Delay Awareness	16.6	10.2	71.4	0.020

Table 4.15: GBR_GAMING Performance With Fading

GBR_NON_CONV_VID			Maximum QoS Delay: 300ms	
	Mean Delay(ms)	Standard Deviation(ms)	Maximum Delay(ms)	Probability Over
Proposed Algorithm	141.9	32.13	262.0	0.063
Proportional Fair + Delay Awareness	116.0	21.8	226.5	0.029

Table 4.16: GBR_NON_CONV_VID Performance With Fading

NGBR_VID_TCP			Maximum QoS Delay: 300ms	
	Mean Delay(ms)	Standard Deviation(ms)	Maximum Delay(ms)	Probability Over
Proposed Algorithm	225.4	38.0	379.7	0.233
Proportional Fair + Delay Awareness	113.3	22.6	220.4	0.029

Table 4.17: NGBR_VID_TCP Performance With Fading

For this simulation, the channel quality was varied for each user and an average taken. This allowed all users to experience favorable and unfavorable conditions. The proposed algorithm places a higher emphasis on the the GBR traffic. This has a negative effect on the NGBR traffic. The α and β terms allow the balance of the two. These values changed due to the change in channel characteristics.

4.4 Overall Result

By utilizing the α and β terms, the proposed algorithm was able to effectively balance the QoS delay restraints of GBR traffic and NGBR traffic. Because there is limited bandwidth, the improved performance of the GBR traffic came at the cost of the NGBR traffic. Although there was a decrease in performance, the NGBR traffic was able to remain under the delay constraint up to 89% of the time. The α and β terms allowed this as there is a trade off between how closely the algorithm weights the delay aware aspect and the proportional fair.

4.5 Assumptions

In order to obtain the results, some assumptions needed to be made. The first is that the eNB is able to transmit to each of the UE separately. If this was not true then each time the eNB stopped transmitting, all of the queues would grow by the amount of time the eNB was not transmitting for. This increase would not be able to be reduced without the eNB using more RBs. This would be a serious assumption to break. The next assumption was that all of the UE were equidistantly placed around the eNB. If the UE were all placed very close together, their transmissions would be required to cease at the same time. If this were violated, a situation similar to the first assumption would be present. As long as there is reasonable spacing between the UE, this is not as serious. Another assumption is that the radar is perfectly periodic without side lobes, that should not be interfered with or cause interference. This would lead to different pattern of eNB transmission stoppage. The model also assumes that all UE are stationary. If this were violated, when the eNB stopped transmitting to each UE would constantly change. This could lead to interference with the radar beam if the eNB transmission did not stop at the proper time.

Chapter 5

Conclusions and Future Work

5.1 Conclusion

In conclusion a radar-aware scheduling algorithm was created. NS-3 was used to simulate a wireless situation in which a radar was simulated. This discrete network simulator was used to simulate the LTE stack and the IP stack. The proposed algorithm was able to successfully balance the QoS requirements of GBR and NGBR traffic. Without fading present, the proposed algorithm had minimal degradation in NGBR quality, with a large increase in quality to the GBR traffic. In the case of fading, the NGBR traffic performance suffered more, but the increase to GBR traffic was still present. This algorithm can allow more efficient use of the CBRS band in the densely populated coastal areas. This allows users to experience higher quality wireless communications.

5.2 Future Work

Future work could include using a more complex model for the radar. The model used was simple and actual radar is more complex than the moving average used. The α_j term and β_j term could be optimized for each individual QCI. Currently the algorithm was tested using a variety of values for the α_j and β_j for the GBR and NGBR traffic. Other antenna models could be used and explored to show their effect

on transmissions. Another future exploration could be adding mobility to each of the UE. This would be more realistic and also require the UE to take the current and next position of the UE to determine when to stop transmitting, as to not interfere with the radar beam.

Bibliography

- [1] 3GPP, “Evolved Universal Terrestrial Radio Access (E-UTRA); Physical layer procedures ,” 3rd Generation Partnership Project (3GPP), Technical Specification (TS) 36.213, 10 2014, version 12.3.0. [Online]. Available: https://www.etsi.org/deliver/etsi_ts/136200_136299/136213/12.03.00_60/ts_136213v120300p.pdf
- [2] ns 3 Project, “Lte module - design documentation.” [Online]. Available: <https://www.nsnam.org/docs/models/html/lte-design.html>
- [3] M. A. McHenry, P. A. Tenhula, D. McCloskey, D. A. Roberson, and C. S. Hood, “Chicago spectrum occupancy measurements & analysis and a long-term studies proposal,” in *TAPAS '06*, 2006.
- [4] J. Mitola, G. Q. Maguire *et al.*, “Cognitive radio: making software radios more personal,” *IEEE personal communications*, vol. 6, no. 4, pp. 13–18, 1999.
- [5] “2011 to 2015 american community survey.” [Online]. Available: <https://www.census.gov/acs/www/data/data-tables-and-tools/data-profiles/2015/>
- [6] L. E. S. G. Locke and A. Secretary, “An assessment of the near-term viability of accommodating wireless broadband systems in the 1675-1710 mhz 1755-1780 mhz 3500-3650 mhz and 4200-4220 mhz 4380-4400 mhz bands,” October 2010.
- [7] “Mathematical models for radiodetermination radar systems antenna patterns for use in interference analysis,” Recommendation, ITU-R M.1851, Tech. Rep., Jun. 2009.
- [8] 3GPP, “Citizens Broadband Radio Service (CBRS) 3.5 GHz band for LTE in the United States,” 3rd Generation Partnership Project (3GPP), Technical Specification (TS) 36.744, 01 2017, version 14.0.0. [Online]. Available: <https://portal.3gpp.org/desktopmodules/Specifications/SpecificationDetails.aspx?specificationId=3103>
- [9] —, “Group radio access network; physical channel and modulation (release 8) ts 36.211,” 3GPP, Tech. Rep., 2009.
- [10] “Ongo wireless coverage - in-building, public space & industrial iot: Cbrs alliance,” Oct 2019. [Online]. Available: <https://www.cbrsalliance.org/>
- [11] S. Sesia, I. Toufik, and M. Baker, *Multi-User Scheduling and Interference Coordination*. Wiley, 2011, pp. 279–292. [Online]. Available: <https://ieeexplore.ieee.org/document/8045774>
- [12] N. Nurani Krishnan, N. Mandayam, I. Seskar, and S. Kompella, “Experiment: Investigating feasibility of coexistence of lte-u with a rotating radar in cbrs bands,” in *2018 IEEE 5G World Forum (5GWF)*, 07 2018, pp. 65–70.

- [13] Q. Zhao, L. Tong, A. Swami, and Y. Chen, “Decentralized cognitive mac for opportunistic spectrum access in ad hoc networks: A pomdp framework,” California Univ Davis Dept. of Electrical and Computer Engineering, Tech. Rep., 2007.
- [14] J. Li, B. Xu, Z. Xu, S. Li, and Y. Liu, “Adaptive packet scheduling algorithm for cognitive radio system,” in *2006 International Conference on Communication Technology*, Nov 2006, pp. 1–5.
- [15] H. T. Friis, “A note on a simple transmission formula,” *Proceedings of the IRE*, vol. 34, no. 5, pp. 254–256, 1946.
- [16] 3GPP, “Universal Mobile Telecommunications System (UMTS);LTE; Architecture enhancements for non-3GPP accesses,” 3rd Generation Partnership Project (3GPP), Technical Specification (TS) 36.402, 11 2014, version 11.4.0. [Online]. Available: https://www.etsi.org/deliver/etsi_ts/136200_136299/136213/12.03.00_60/ts_136213v120300p.pdf